

The First VisAO Fed Integral Field Spectrograph: VisAO IFS

Katherine B. Follette^{*a}, Laird M. Close^a, Derek Kopon^a, Jared R. Males^a, Victor Gasho^a,
Kevin M. Brutlag^a, Alan Uomoto^b

^aCAAO, Steward Observatory, University of Arizona, Tucson, AZ, USA 85721

^bOCIW, 813 Santa Barbara St., Pasadena, CA, USA 91101

ABSTRACT

We present the optomechanical design of the Magellan VisAO Integral Field Spectrograph (VisAO IFS), designed to take advantage of Magellan's AO system and its 85.1cm concave ellipsoidal Adaptive Secondary Mirror (ASM). With 585 actuators and an equal number of actively-controlled modes, this revolutionary second generation ASM will be the first to achieve moderate Strehl ratios into the visible wavelength regime. We have designed the VisAO IFS to be coupled to either Magellan's LDSS-3 spectrograph or to the planned facility M2FS fiber spectrograph and to optimize VisAO science. Designed for narrow field-of-view, high spatial resolution science, this lenslet-coupled fiber-fed IFS will offer exciting opportunities for scientific advancement in a variety of fields, including protoplanetary disk morphology and chemistry, resolution and spectral classification of tight astrometric binaries, seasonal changes in the upper atmosphere of Titan, and a better understanding of the black hole M-sigma relation.

Keywords: Adaptive optics, VisAO, Magellan, IFS, IFU

1. INTRODUCTION: INTEGRAL FIELD SPECTROSCOPY

Integral Field Spectroscopy is a method for simultaneously acquiring data across one spectral and two spatial dimensions. What results is a 3-D data cube that can be used to study composition gradients across extended sources (disks, jets, nebulae) as well as to separate and classify objects in densely packed fields (globular cluster and galaxy cores, tight binaries). IFS data cubes can be sliced to create 2-D maps of science targets in a particular spectral feature or in a particular line ratio. IFS data collection is also exceptionally tunable, as an observer may choose to bin either spatially or spectrally depending on their particular science requirements.

There are currently more than twenty astronomical IFSs in operation, including one on each of the 8m class telescopes (Keck, Gemini, Subaru, Magellan and the VLT), and IFS modes have been incorporated into several recent space telescope designs, including those of JWST and Herschel. While IFS data reduction proved prohibitively complicated for the non-specialist when the technology was in its infancy, much emphasis has since been made on the outlining of standard reduction techniques and software routines, and IFS data are now fully incorporated into the general astronomer's data "toolbox".

1.1: Fiber-fed IFUs

A fiber-fed IFU consists of a fiber bundle placed at the focal plane of the telescope and arranged on the other end into a pseudo-slit to be fed to the spectrograph. All IFS designs containing optical fibers suffer from a phenomenon called Focal Ratio Degredation (FRD). The acknowledged primary cause of FRD is internal scattering within the fibers, but the precise physical scattering mechanism is still widely debated in the literature. Stress on the fibers can further add to FRD, however that effect can be minimized with proper polishing and cabling techniques. Fibers also suffer from azimuthal scrambling, which proves to be both a blessing and a curse in terms of data quality. On one hand, it increases the entropy of the beam and results in information loss, however it also smooths out the effect of optical aberrations, effectively symmetrizing the beam. A fundamental advantage of fibers is that, if well-manufactured, they can have 95% throughput or greater, surpassing even a mirror freshly coated with aluminum, which is only 92% reflective¹.

If fibers act as the primary light collectors, they have a maximum fill factor of approximately 65% of the focal plane due to gaps between fibers (which must be cladded to prevent leakage). If that fill factor is sufficient, a direct

* kfollette@as.arizona.edu; phone: 520-621-6523

fiber-fed system will maximize the throughput and minimize scattering surfaces in the optics. However, if truly “integral” sampling of the science field is a priority, as it is in the case of VisAO IFS, an array of microlenslets may be fabricated to feed only the very core of each optical fiber. This adds an additional scattering surface and therefore results in an inherently lossier beam, however the microlenslets are generally fabricated to fit flush with one another so as to fully sample the focal plane. The lenslets also allow for more control over the input and output f-ratio of the beam, which can be tailored to minimize FRD. The addition of a lenslet array to the optical system lowers the throughput from ~95% for fibers alone to 60-70% for lenslet and fiber systems². However, this tradeoff is acceptable in the case of VisAO IFS because the VisAO system is best suited to the study of fairly bright science targets where loss of signal is not a concern. It is also often necessary to add a second microlenslet array at the fiber output in order to slow down the beam exiting the fiber (sped up in the fiber due to FRD) to the desired input f-ratio of an existing spectrograph. In our case, this second lenslet array can be tailored to suit either the facility LDSS-3 spectrograph's f/11 beam or the M2FS spectrograph's beam, currently in the design process.

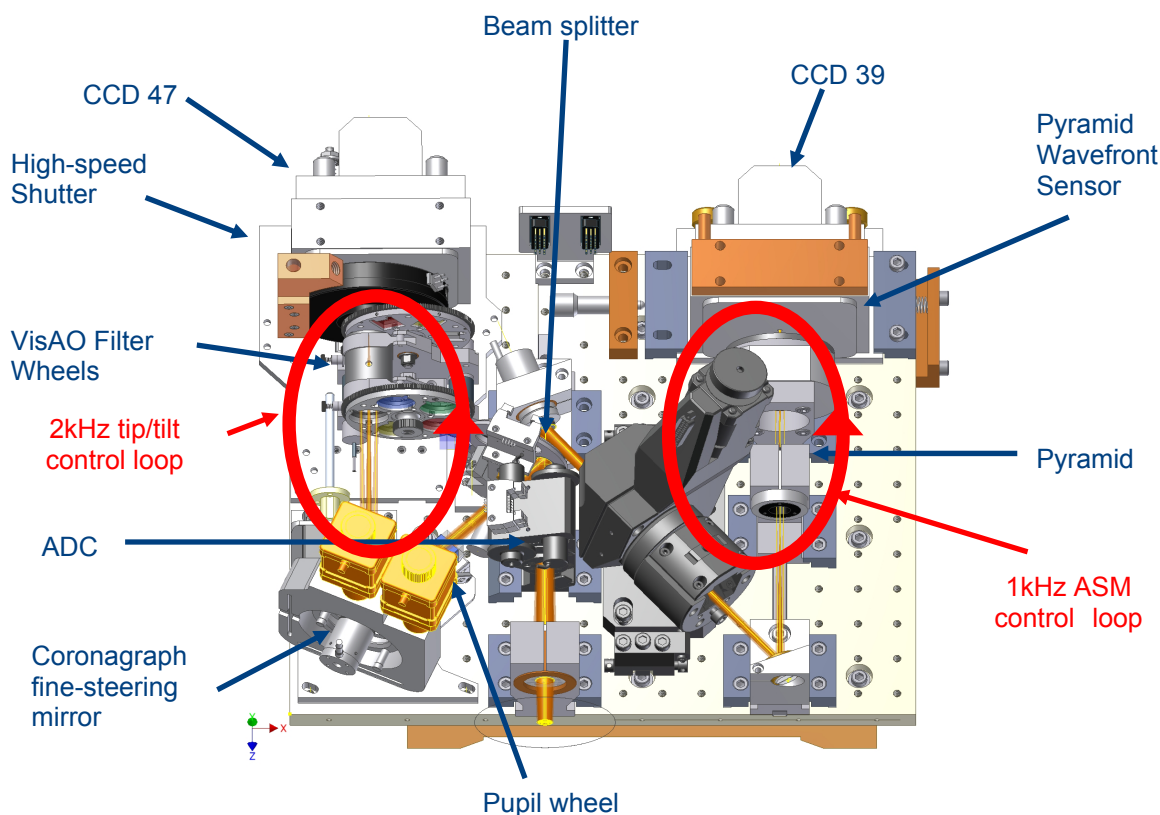


Figure 1. The mechanical design of the Magellan VisAO system, with the key features for visible AO science indicated by blue arrows. The red loops indicate the two control loops for wavefront correction. Light from the ASM enters from the bottom.

2. THE MAGELLAN VISAO SYSTEM

The MagAO IFS is a direct result of the development of the Magellan VisAO system, so before discussing the IFS design, an understanding of the basic structure of the VisAO system is necessary. Perhaps the most important and unique feature of the VisAO system is built right into its name. It is, first and foremost, a system designed to make use of the exceptionally high number of controllable modes of the Magellan ASM, which map to a 23cm pitch on the 6.5m primary mirror, in order to push Adaptive Optics into the visible wavelength regime. An overview of the VisAO system design can be found elsewhere in these proceedings³.

Using scalings from the currently operational MMT ASM, we can estimate that the Magellan system will approach ~68% Strehl at H band and ~15% Strehl at 0.7 μm in 0.7" seeing. This simple scaling argument provided early

evidence that the ASM was capable of moderate correction shortward of the NIR, however such scalings will not suffice as proof of concept, so we have conducted simulations of VisAO performance using the Code for Adaptive Optics Simulation^{4,5}, an IDL-based simulation environment designed specifically for adaptive optics.

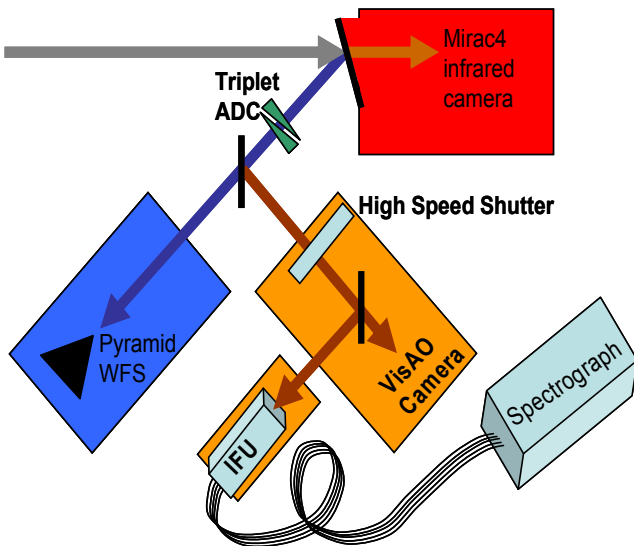


Figure 2: Schematic of the Magellan VisAO system, showing the key components for VisAO science: the Pyramid WFS, the Triplet ADC, the High Speed Shutter, the VisAO Camera and VisAO IFS.

Using a 6-layer atmospheric model derived from atmospheric surveys at Las Campanas, and Arcetri Group documentation of LBT ASM simulations as a guide, simulated AO images are created at visible wavelengths. These simulated images are scaled to the true obscured Magellan PSF, and 30nm RMS plus 30nm non-common path errors are inserted to produce the mean Strehl ratio vs. guide star R magnitude plot shown in Figure 3 (median 0.7" seeing conditions are assumed). Note that moderate Strehls are achievable out to guide star magnitudes of 9 or 10, after which Strehl drops precipitously. As such, VisAO IFS science has been designed to make use of targets with bright nearby Natural Guide Stars (NGS).

As a further proof of concept, closed-loop tests of the LBT ASM (of which the Magellan ASM is a clone) have proven that their system is capable of producing 25% SR at 0.7 μ m and under 0.7" seeing conditions (see Figure 4). Furthermore, recent on-sky testing of the currently installed LBT ASM have shown it capable of achieving 50-60% SR at H band.⁶

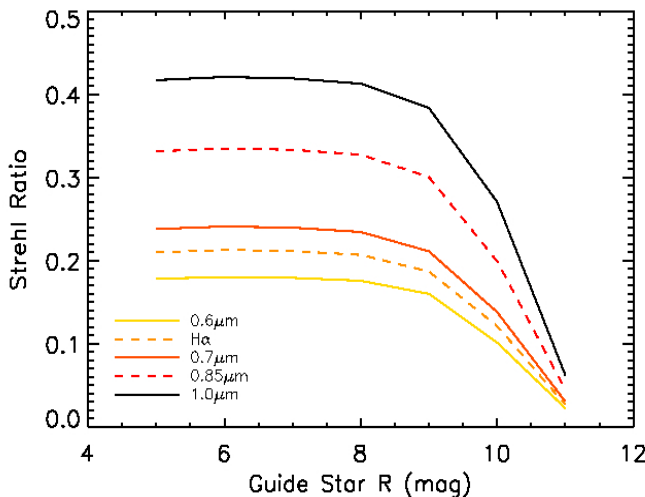


Figure 3: Numerical simulations (with measured Strehls) of the VisAO Strehl ratio vs. guide star R magnitude. For R < 9 mag we will achieve SR > 0.2 in the R band.

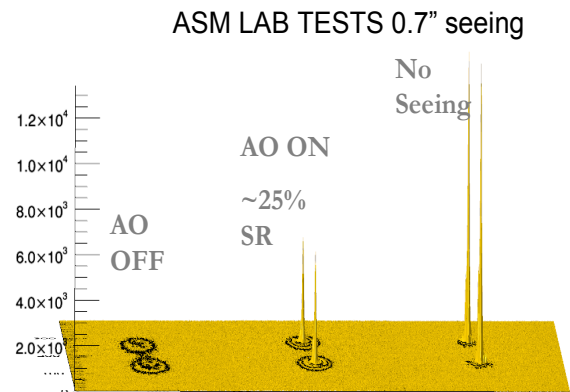


Figure 4: Real closed loop "end-to-end" lab tests of a clone system (LBT1, 400 modes, 1 kHz) in the ASM test tower at Arcetri Observatory in Florence, Italy. The image shows a simulated binary star with AO off (SR~0) and with AO on (25% Strehl at 0.7 μ m). These AO images were obtained with 400 modes and 0.7" simulated seeing. The filter used is a broad-band R filter.

3. VISAO IFS OPTICAL DESIGN AND SPECTROGRPH

The VisAO IFS components are such that they can currently be modified to feed any facility spectrograph at its desired input f-ratio. The project currently has two good options for spectrographs into which a VisAO IFS fiber feed can be plugged: the facility LDSS3 spectrograph, and the new M2FS spectrograph, which is under construction.

3.1: VisAO IFS + LDSS-3⁷

With the scientific goal of bright source, high spatial resolution science, we designed the MagIFU+LDSS-3 system to make maximal use of LDSS3's 12.9' longslit. Our primary science goal was to make the finest possible spatial sampling, so we first sought out the smallest multi-mode "astronomy-class" fibers available, settling on fibers with a 50 μ m core and 125 μ m of cladding. Since maximal fill-factor was also a priority for VisAO IFS science, we decided on a lenslet+fiber design, with a microlenslet that refocuses each spaxel into a ~26 μ m "spot" at the center of each 50 μ m fiber core. This custom 26 by 26 square microlenslet array has a 99% fill-factor and a 160 μ m pitch between lenslets. It will be carefully epoxy bonded (UV cured) to match the 26x26 grid of fibers, which will be held in a custom silicon etched "jig" and aligned to better than 5 μ m. In order to preserve both sensitivity and a sufficient FOV, 20mas was decided to be the optimal scale for the finest spatial sampling mode of VisAO IFS. Two removable lens triplet may be inserted into the beam as shown in figure 6a to slow the f/48 VisAO beam to f/225, providing the desired fine spaxel scale and spots shown in Figure 6b.

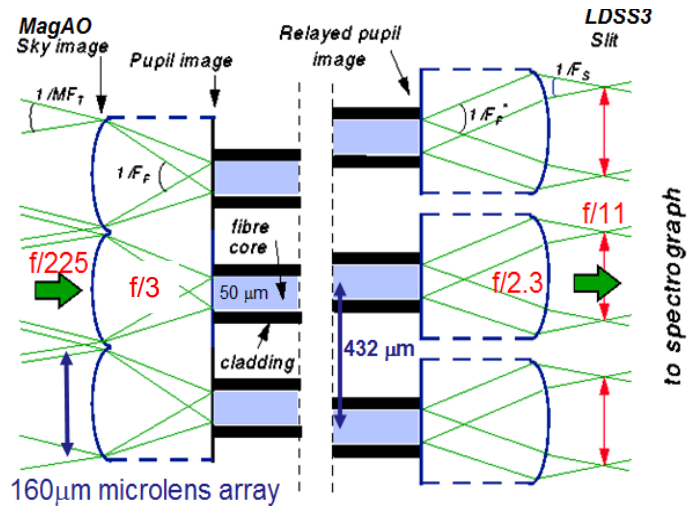


Figure 5: A schematic diagram of the input and output fiber+lenslet design to couple the LDSS3 slit to the MagAO focal plane with 20mas spaxials. The $f/225$ beam is modified to $f/3$ by a custom 26 x 26 microlenslet array, with each lenslet feeding a 50 μ m fiber core. The beam passes out of the fiber at $\sim f/2.3$ due to FRD and is modified to the desired $f/11$ input for LDSS-3 with a second custom linear lenslet array Modified from <http://star-www.dur.ac.uk/~jra/integral field.html>.

As with most other Astronomical IFS designs, a coarser spatial sampling mode is also desirable to optimize light collection for fainter, extended sources that cannot be detected in the 20mas mode. If the two triplet lenses are not inserted into the beam, the original $f/48$ beam is focused on the input lenslet. In this "coarser" mode, each lenslet subtends a 105x105 mas spaxel on the sky.

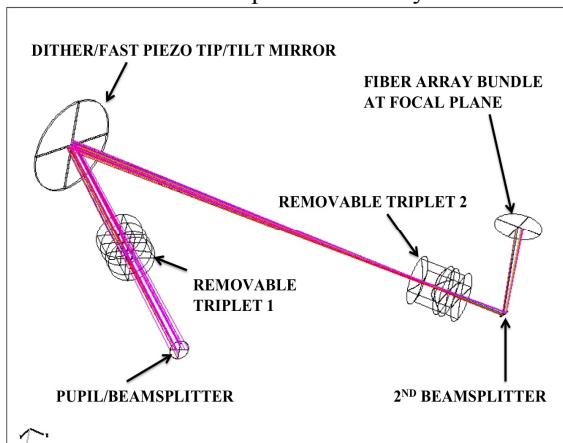


Figure 6a The $f/225$ (20mas spaxel) input beam optical design, with two removable triplet lenses.

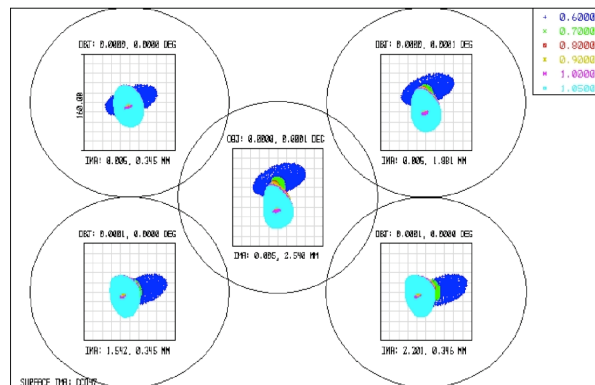


Figure 6b. Spot diagrams of the VisAO focal plane (fiber head) in 20mas mode. The circles are the first Airy minimum at 0.6 μ m and the squares are the size of a lens element (160 μ m by 160 μ m)

The 50 μm exit “pupils” formed by each fiber are reimaged to form a slit. LDSS-3 requires an $f/11$ input beam, however the output of the fibers will be approximately $f/2.3$ due to FRD. Slowing of the beam to $f/11$ will be accomplished through use of 26 custom fast 26x1 microlenslet linear arrays that will be aligned to form a custom LDSS-3 slit mask as shown in Figure 7.

The 26 by 26 spaxel design was chosen to optimize the use of the LDSS-3 slit, which will see 676 $f/11$ “stars”. The spacing between feeds was chosen to be twice the FWHM of a 0.7” seeing “star” spot, which amounts to 6 pixels of separation between each of the 676 spectral traces on the LDSS3 40962 CCD.

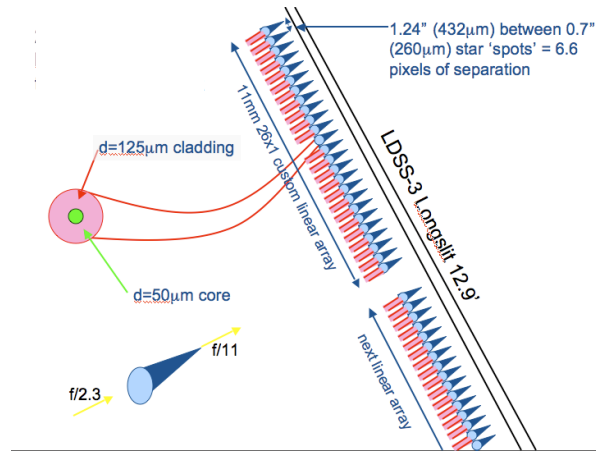


Figure 7. 26 26x1 custom linear lenslet arrays will plug into the LDSS-3 longslit

3.2 Design compatibility with other facility spectrographs

Customization of VisAO IFS design to be compatible with the LDSS-3 spectrograph is inherent only in the design of the final input linear lenslet array, which is not yet fabricated. By modifying just this backend piece, the VisAO IFS design could be made compatible with nearly any other spectrograph. Magellan is planning to add another facility spectrograph, M2FS, and our design can be easily modified to accommodate plugging into it instead of LDSS-3. M2FS, currently in the design stage and being led by PI Mario Matteo at the University of Michigan, is being designed as a fully fiber-fed system with low resolution modes of comparable spectral resolution to LDSS-3 as well as a high resolution echelle mode with spectral resolutions of up to $R \sim 22,000$.

4. DESIGN CONSIDERATIONS FOR OPTIMAL DATA QUALITY

As an optical, AO-fed IFS, the VisAO IFS has four primary barriers to overcome in order to achieve optimal data quality.

4.1 Differential atmospheric refraction (DAR)

The Earth’s atmosphere refracts incoming starlight by an amount that varies with wavelength. As such, light of different wavelengths coming from the same point in space will be spread by the earth’s atmosphere into a mini-rainbow of colors. This results in radial scrambling of an incoming IFS signal and must therefore be corrected to preserve full spatial accuracy. Correction for DAR can be applied as a final step in the reduction of IFS data, however it is cleaner to correct for DAR upstream of the IFS through the use of an optic called an Atmospheric Dispersion Corrector (ADC).

Most ADCs designed and built to date consist of two identical counter-rotating prism doublets (often referred to

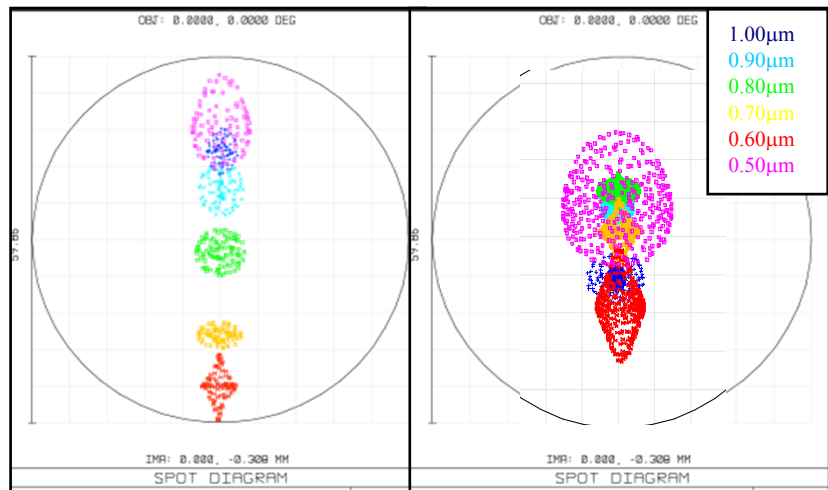


Figure 8. Spot diagrams for a conventional 2-doblet ADC (left) and our advanced 2-triplet ADC (right) at 1.55 airmasses (50 degree zenith angle). The spot size is $>58\%$ smaller for the 2-triplet design.

as Amici prisms) made of a crown and flint glass. The indices of the two glasses are matched as closely as possible in order to avoid steering the beam away from its incident direction as the components rotate. The wedge angles and glasses of the prisms are chosen to correct primary chromatic aberration at the most extreme zenith angle. By then rotating the two doublets relative to each other, an arbitrary amount of first-order chromatic aberration (lateral color) can be added to the beam to exactly cancel the dispersion effects of the atmosphere at a given zenith angle. The standard 2-Doublet design corrects the atmospheric dispersion so that the longest and shortest wavelengths overlap each other, thereby correcting the primary chromatism. Secondary chromatism is not corrected and is the dominant source of error at higher zenith angles. To correct higher orders of chromatism, more glasses and thereby more degrees of freedom are needed

In our 2-triplet design⁸, a third glass with anomalous dispersion characteristics (Schott's N-KZFS4) is added to the crown/flint pair. Like the doublet, the index of the anomalous dispersion glass was matched as closely as possible to that of the crown and flint. The Zemax atmospheric surface was set to 70° zenith and the relative angles of the ADC were set to 180°. The wedge angles of the three prisms in the triplet were then optimized to correct both primary and secondary chromatism.

Using the on-axis rms spot size over the broad band 0.5-1.0 μm as the figure of merit, our 2-triplet performs >58% better at high airmass (>1.5 AM) than a conventional 2-doublet design (compare figure 8a to 8b). This will allow diffraction-limited broadband imaging at the VisAO focal plane and much better pyramid WFS performance. It also eliminates the need for DAR correction in the IFS data pipeline.

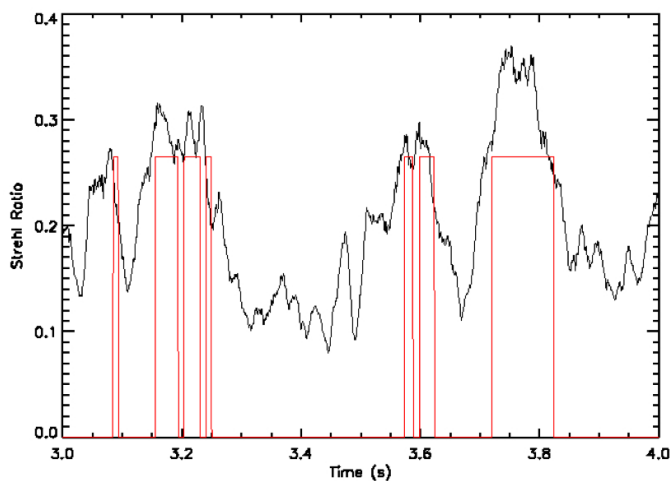


Figure 9. Simulated SR at 0.7 μm, with shutter position overlaid. The red line shows the shutter opening mostly while SR is above the threshold of 0.3.

4.2 Rapidly variable visible Strehl ratios

Although the mean SR of Magellan VisAO images is expected to be ~20% in R band, rapidly variable seeing in the visible wavelength regime is expected based on simulations, with temporary peak SRs of as high as 50%. This variability can be seen in Figure 9, which shows a prediction of the variation in SR over a period of 1 second at 0.7 μm. In order to take advantage of these brief periods of high Strehl, we have designed a high speed shutter which uses real-time frame selection techniques to expose only during periods of high SR by predicting image quality a few ms in advance, enough time to open or close the shutter. The shutter has been acquired and is functioning in the lab, and the prediction accuracy of the initial real time frame selection algorithm is 95%. This technique is similar to "Lucky Imaging", however it does not require an Electron-Multiplying CCD (EMCCD) for science imaging and so allows for longer exposures and therefore lower readout noise.⁹

4.3 Accurate PSF subtraction

In order to achieve accurate PSF calibration, the fold flat that reflects the VisAO beam into the IFU optical path is only 95% reflective. The final 5% of the beam passes through the flat to the CCD47, which is used here as a guider rather than a science camera. This allows us to obtain simultaneous PSF calibration images and IFS science data. In this setup, the CCD47 will also function as a tip/tilt sensor and will run at 2kHz in order to correct residual wavefront errors.

4.4 Focal ratio manipulation

On the whole, the optomechanical design of VisAO IFS introduces a number of additional scattering surfaces into the optics that will result in significant losses. However, the limit on guide star magnitude and need for it to lie

within the small IFS FOV for AO functionality already biases us towards bright sources. Loss of signal on these bright sources is therefore not our primary concern.

5. SELECTED SCIENCE CASES FOR AO-CORRECTED VISIBLE IFS SCIENCE

It is paramount that the VisAO IFS be optimized from the start to answer interesting astrophysical questions. We must be careful to design the instruments and the science to be “self-calibrating”, so as not to be hampered by the moderate to low Strehls expected in the visible. We present very briefly a few interesting new science cases that are enabled by the highest spatial resolution mode of the IFS.

5.1 Herbig Ae/Be disks

The unprecedented combination of spatial and spectral resolution in the optical provided by VisAO IFS will open up an exciting frontier in the study of Herbig Ae/Be circumstellar disks (almost all of which are good $R < 11$ mag guide stars). According to recently published models, photoionized disk atmospheres are expected to radiate detectable amounts of forbidden line emission¹⁰. The [OI] 6300 Angstrom line has been spectrally resolved in such disks with UVES on the VLT¹¹, however spatial information can currently only be estimated through careful modeling of these ultra-high-resolution spectra. The ability to spatially resolve features such as gaps, jets and flaring would aid greatly in our understanding of disk structure and its connection to the process of planet formation. The “trick” here is that the hot star is pure continuum at 6300A, so simple continuum subtraction will reveal the disk (and or jet) in emission at each spaxial without

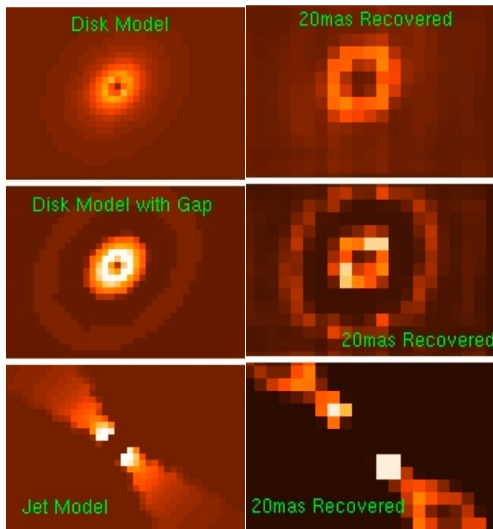


Fig 11: Disk, gap, and jet models (left) vs. 20 mas/pix IFU [OI] images (right; just the inner 20x14 spaxels) with correct S/N for 1 hr. int. on HD101412’s ~10 AU radius disk.

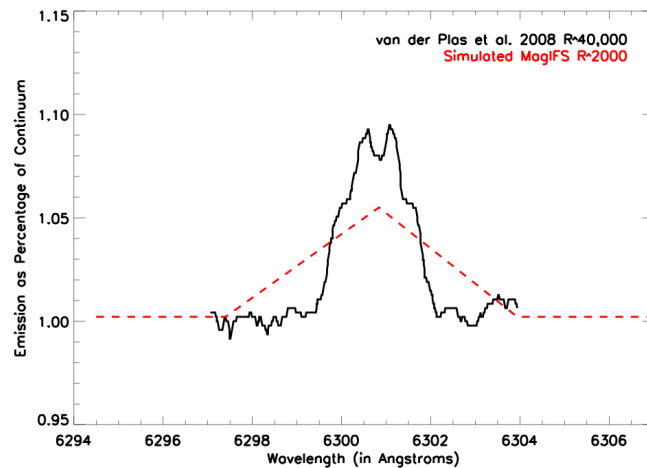


Figure 10. The spectrum of HD101412 as observed by van der Plas et al (2008) is shown in black, and the simulated VisAO IFS spectrum with $R \sim 2000$ in red. This shows that the [OI] line at 6300A is recoverable with a lower resolution spectrograph at $\sim 5\%$ above the continuum.

contamination from the star. We investigated the suitability of our proposed instrument to attack the question of disk morphology with a preliminary study of the type of disk structure resolvable with a diffraction-limited optical IFS. We began by binning the spectra of van der Plas et al to a lower ($R \sim 2000$) spectral resolution in order to verify that the line would be visible at low resolution as an appreciable fraction of the continuum. The results, shown in Figure 10, show that while kinematically unresolved, the line is still detectable at $R \sim 2000$. Furthermore, the high spatial resolution of VisAO IFS makes high spectral resolution unnecessary in order to understand the disk morphology.

One might imagine that another barrier to detectability of forbidden line emission from such disks would be the smaller size of the Magellan telescope compared to the 8m VLT as well as the greater multiplexing of VisAO IFS (as the signal is divided into 676 pieces). However our lower spectral resolution is an advantage in terms of signal collection. Using aperture and sensitivity scalings, we estimate that it will indeed take a longer (approximately 1 hour) but not unfeasible amount of time to achieve $SNR \sim 100$ VisAO IFS spectra of such disks.

To investigate our ability to resolve structure in Herbig Ae/Be disks, we simulated a protoplanetary disk around a typical Herbig Ae/Be star at the distance of the Taurus-Auriga star forming region using smoothed versions of the radial profiles inferred by van der Plas et al. The ability of the instrument to resolve visible wavelength forbidden lines in the atmosphere of a disk was examined for three feasible geometries: a disk, a disk with a gap from 5-10AU and a jet.

Figure 11 shows simulated [OI] 6300Å images of these three cases. The stellar continuum is easily isolated in spectral space with the IFU (through the “trick” described above), and has been subtracted from each IFU spaxial. Each spaxial represents one fiber and is 20x20mas on the sky, making a spectrum from 0.6-1.05 mm with $R \sim 1800$. The lefthand panel of Fig. 4 shows the theoretical disk model, while the righthand shows the final deconvolved [OI] disk image ($SR=15\%$). In each case, the real features in the disk are easily recovered and distinguished from one another. PSF knowledge will be excellent through simultaneous use of the 8.5mas/pix VisAO camera (redirecting $\sim 5\%$ of the IFU light for PSF calibration).

Anticipating cases in which a young star might exhibit forbidden line emission from both a circumstellar disk and a jet (particularly at the [SII] 6716, 6731 Angstrom “jet” lines), we also created a hybrid disk/jet model with a variety of brightness scalings between the two components. Shown in Fig. 12 is one such recovered spatial map of a simulated system in which the jet is 10 times brighter than the disk. Even with such contrast, the disk is still recoverable. This suggests that the VisAO IFS will be a uniquely powerful tool for understanding jet creation and collimation and the structure of protoplanetary disks. In fact, we can probe any variety of emission line system (given a bright enough NGS) at 20 mas resolution, including ultra compact HII regions, planetary nebulae, and propylids.

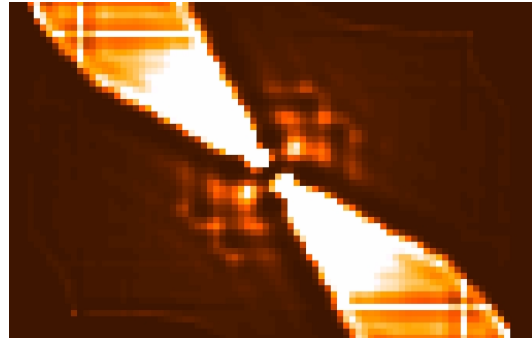


Fig 12: Simulated IFU [OI] jet and $r \sim 10$ AU disk image (1 hr. integration)

5.2 Resolved spectra of tight astrometric binaries

We have also examined the feasibility of resolving tight astrometric binaries and classifying the spectral type of each member of the binary pair. We found 341 candidates for such a study in the U.S. Naval Observatory’s Sixth Orbital Ephemerides Catalog. Each candidate binary system has a declination less than $+40^\circ$, a V magnitude between 5 and 11 for each component and a V magnitude difference of less than 2 between components. Each system has calculated astrometric orbits that leave the components with a separation of less than one arcsecond in the 2011 epoch. In fact, the vast majority of these known astrometric binaries (330/341) have separations under 0.2 arcseconds and cannot be spectrally resolved with current speckle or interferometric techniques. An IFU with high spatial resolution in the visible will allow for the first unambiguous spectral classification of each component of these 330 binaries. Accurate temperatures (when combined with the known dynamical masses of each system) will lead to a better understanding ($\sim 1-5\%$ accuracy) of the fundamental high-mass end of the mass-temperature-luminosity relations.

5.3 Asteroid and solar system surfaces and Titan’s atmosphere

There are many science cases where simply mapping objects at these very high resolutions is exciting. For example, the IFU can map Titan (diameter $\sim 0.7''$) through the $0.95\mu\text{m}$ CH_4 window during its shift from northern winter to summer. This seasonal shift is expected to induce evaporation of hydrocarbon lakes found there by Cassini, which should have observable effects on Titan’s atmosphere and surface. The IFS can, in fact, be used to map the surface of any bright solar system body at a particular visible wavelength, including asteroid surfaces, the Galilean moons, and most planets.¹²

5.4 AGN and black holes

The extragalactic science cases for the VisAO IFS high-resolution mode include a study of all of the nearby AGN (and their surrounding stellar populations) on which we can guide, including NGC 1068. Such a study would

provide the highest optical spatial resolution to date in the region of dynamical influence of the central black hole, and may aid in our understanding of the mysterious relationship between central black hole masses and the velocity dispersions of the galactic bulges that host them.^{13,14} We have also developed a case for looking at the very dense cores of globular clusters. A better understanding of the 3D kinematics of such regions (which is possible even with our low spectral resolution) could help provide evidence for or rule out the existence of black holes at their centers.

6. COMPARISON TO GMOS

In order to demonstrate the niche of visible-wavelength regime, high-spatial resolution science carved out by VisAO IFS, we will compare it here to another widely used optical IFS: The Gemini Multi-Object Spectrograph (GMOS). In IFS mode, GMOS uses a 1500 element fiber-coupled hexagonal lenslet array which is divided into 1000 science spaxels and a 500 element sky field located 1' away from the science field. The Gemini ALTAIR AO system feeds the science instruments at a minimum wavelength of 0.835 μ m and does not provide any correction outside of the IR. There are plans to increase the red-sensitivity of GMOS into the IR in order to take advantage of ALTAIR's capabilities. However, with 177 controllable modes for the ALTAIR DM, AO capability cannot be pushed into the visible regime on Gemini.

GMOS was designed to do Integral Field Spectroscopy on significantly larger, fainter sources than VisAO IFS. As such, its spaxels are 0.2" each, 10 times larger than the VisAO IFS spaxels. This propensity toward the study of extended sources also makes its offset sky field a true asset, whereas VisAO IFS science targets are generally compact enough to provide a sufficient sky region within the field itself. In cases where VisAO IFS science targets are extended enough to occupy most of the FOV, separate sky frames will need to be obtained.^{15,16}

7. CONCLUSION

We feel that the addition of VisAO IFS, which has been funded through the design stage, to the instruments available to the astronomical community will open up scientific regimes currently inaccessible by even the most sophisticated IFS. In keeping with the NSF's AO Roadmap goal of opening pathways to "large aperture telescope visible AO instrumentation and science", development of Magellan's VisAO system and IFS are an important step on the path to widespread VisAO science. The technologies developed for this first-generation VisAO system will provide unprecedented spatial resolution in the optical, allowing for the probing of many heretofore unanswered scientific questions and likely the raising of many more, guiding future VisAO instrument development.

REFERENCES

- [1] Bershady, M., [3D Spectroscopy in Astronomy, XVII Canary Island Winter School of Astrophysics] Cambridge University Press, (2009).
- [2] Poppett, C. L. and Allington-Smith, J. R., "The dependence of the properties of optical fibres on length", MNRAS 404, 1349P (2010).
- [3] Close, L. M., Gasho, V., Kopon, D., Males, J. R., Follette, K., Brutlag, K., Uomoto, A., and Hare, T., "The Magellan Telescope Adaptive Secondary AO System: AO Science in the Visible and Mid-IR," Proc. SPIE 7736, (2010).
- [4] Carillet, M., Vérinaud, C., Femenía, B., Riccardi, A., and Fini, L., "Modelling astronomical adaptive optics - I. The software package CAOS," MNRAS 356, 1263–1275 (2005).
- [5] Carillet, M., Vérinaud, C., Esposito, S., Riccardi, A., Puglisi, A., Femenía, B., and Fini, L., "Performance of the first-light adaptive optics system of LBT by means of CAOS simulations," Proc. SPIE 4839, 131–139 (2003).
- [6] Esposito, S. et al. "First light AO (FLAO) system for the LBT: final integration and acceptance test results in Europe", Proc. SPIE 7736, (2010).
- [7] Kopon, D., Close, L. M., Males, J. R., Gasho, V., and Follette, K., "The Magellan adaptive secondary VisAO Camera: diffraction-limited broadband visible imaging and 20mas fiber array IFU," Proc. SPIE 7736, (2010).
- [8] Kopon, D., Close, L. M., and Gasho, V., "An advanced atmospheric dispersion corrector for extreme AO," Proc. SPIE 7015, (2008).
- [9] Males, J. R., Close, L. M., Kopon, D., Gasho, V. and Follette, K., "Frame selection techniques for the Magellan adaptive optics VisAO camera," Proc. SPIE 7736, (2010).

- [10] Ercolano, B., Drake, J. J., Raymond, J. C. & Clarke, C. C., "V-ray irradiated protoplanetary disk atmospheres. I. Predicted emission-line spectrum and photoevaporation," *ApJ*. 688, 398E. (2008)
- [11] van der Plas, G., van den Ancker, M. E., Fedele, D., Acke, B., Dominik, C., Waters, L. B. F. M. & Bouwman, J., "The structure of protoplanetary disks surrounding three young intermediate mass stars. I. Resolving the disk rotation in the [OI] 6300Å line," *A&A*. 485, 487V (2008).
- [12] Schaller, E. L., Brown, M. E., Roe, H. G., Bouchez, A. H., Trujillo, C. A., "Dissipation of Titan's south polar clouds," *Icarus*. 184, 517S. (2006).
- [13] Ferrarese, M. & Merritt, D., "A fundamental relation between supermassive black holes and their host galaxies," *ApJ* 539, 9F (2000).
- [14] Gebhardt et al., "A relationship between nuclear black hole mass and galaxy velocity dispersion," *ApJ* 523, 13G (2000).
- [15] Allington-Smith et al., "Integral field spectroscopy with the Gemini multiobject spectrograph. I. Design, construction and testing," *PASP*. 114, 892A. (2002).
- [16] Westmoquette et al., "The IFS Wiki", <http://ifs.wikidot.com/welcome>, (2010)